농학박사학위논문

*Fusarium graminearum*의 전사조절인자 RFX1의 기능연구

Transcription factor RFX1 is critical for maintenance of chromosome integrity in *Fusarium graminearum*

2014년 8월

서울대학교 대학원

농생명공학부 식물미생물전공

민 경 훈

Transcription factor RFX1 is critical for maintenance of chromosome integrity in *Fusarium graminearum*

A dissertation submitted in partial

fulfillment of the requirement for

the degree of

DOCTOR OF PHILOSOPHY

to the Faculty of

Department of Agricultural Biotechnology

at

SEOUL NATIONAL UNIVERSITY

By

Kyunghun Min

August, 2014

Fusarium graminearum 의 전사조절인자 RFX1 의 기능연구

지도교수 이 인 원

이 논문을 농학박사학위논문으로 제출함
2014년 5월

서울대학교 대학원
농생명공학부 식물미생물전공
민 경 훈

민경훈의 박사학위논문을 인준함
2014년 6월

위 원 장 이 용 환

부 위원장 이 인 원

위 원 이 상 기

위 원 서 정 아

위 원 김 건 철

A THESIS FOR THE DEGREE OF DOCTOR OF PHILOSOPHY

Transcription factor RFX1 is critical for maintenance of chromosome integrity in *Fusarium graminearum*

UNDER THE DIRECTION OF DR. YIN-WON LEE

SUBMITTED TO THE FACULTY OF THE GRADUATE SCHOOL
OF SEOUL NATIONAL UNIVERSITY

BY
KYUNGHUN MIN

MAJOR IN PLANT MICROBIOLOGY
DEPARTMENT OF AGRICULTURAL BIOTECHNOLOGY

June 2014

APPROVED AS A QUALIFIED THESIS OF KYUNGHUN MIN
FOR THE DEGREE OF DOCTOR OF PHILOSOPHY
BY THE COMMITTEE MEMBERS

CHAIRMAN Yong-Hwan Lee

VICE CHAIRMAN Yin-Won Lee

MEMBER Sangkee Rhee

MEMBER Seong-Ah Seo

MEMBER Jin-Cheol Kim

Abstract

Transcription factor RFX1 is critical for maintenance of chromosome integrity in *Fusarium graminearum*

Kyunghun Min

Major in Plant Microbiology

Department of Agricultural Biotechnology

The Graduate School

Seoul National University

The survival of cellular organisms depends on the faithful replication and transmission of DNA. Regulatory Factor X (RFX) transcription factors are well conserved in animals and fungi, but their functions are diverse, ranging from the DNA-damage response to ciliary gene regulation. We investigated the role of the sole RFX transcription factor, RFX1, in the plant-pathogenic fungus *F. graminearum*. Deletion of *rfx1* resulted in multiple defects in hyphal growth, conidiation, virulence, and sexual development. Deletion mutants of *rfx1* were more sensitive to various types of DNA damage than the wild-type strain. Septum

formation was inhibited and micronuclei were produced in the *rfx1* deletion mutants. The results of the neutral comet assay demonstrated that disruption of *rfx1* function caused spontaneous DNA double-strand breaks (DSBs). Transcript levels of genes involved in DNA DSB repair were up-regulated in the *rfx1* deletion mutants. DNA DSBs produced micronuclei and delayed septum formation in *F. graminearum*. GFP-tagged RFX1 localized in nuclei and exhibited high expression levels in growing hyphae and conidiophores, where nuclear division was actively occurring. RNA-sequencing-based transcriptomic analysis revealed that RFX1 suppressed the expression of many genes, including those required for the repair of DNA damage. Taken together, these findings indicate that the transcriptional repressor *rfx1* performs crucial roles during normal cell growth by maintaining genome integrity.

Keywords: Fusarium graminearum, Transcription factor, RFX1, DNA double-strand break, Cell division, RNA sequencing

Student Number: 2008-23080

CONTENTS

LIST OF TABLES

LIST OF FIGURES

INTRODUCTION

The propagation of cellular organisms depends on the accurate replication and transmission of DNA from one cell to its daughters. However, the DNA of organisms is continually subjected to damage from exogenous and endogenous sources. The DNA-damage response has evolved to achieve genome integrity. In response to DNA damage, cells arrest the cell cycle and induce expression of a set of proteins that facilitate DNA repair through a DNA damage responsive signal-transduction pathway. Components of this pathway have been the subjects of intensive investigation in model organisms (1).

ScRFX1 is a transcription factor (TF) in *Saccharomyces cerevisiae* that binds to promoters of target genes involved in DNA repair (2). ScRFX1 recruits the general repressors SSN6 and TUP1 to inhibit the transcription of target genes. In response to DNA damage, MEC1 is activated through an unknown mechanism. Activated MEC1 phosphorylates RAD53 that, in turn, phosphorylates DUN1 kinase. When ScRFX1 is phosphorylated in a DUN1-dependent manner, it loses its DNA-binding capacity. This process leads to the transcriptional activation of target genes, such as ribonucleotide reductases (RNRs). Increased RNR expression facilitates efficient DNA repair because RNRs supply dNTPs, which are precursors for DNA repair (3, 4). Therefore, disruption of ScRFX1 function triggered the de-repression of RNRs that make the cells more resistant to DNA damage (2, 5, 6).

DNA-binding domain of ScRFX1 shares high sequence similarity with those of the animal RFX TF family (2). Lubelsky et al. reported the functional

conservation of RFX from *S. cerevisiae* to humans in response to DNA damage (7). In addition to the DNA-damage response, RFX TFs are central regulators in a transcriptional network regulating ciliary gene expression in sensory neurons (8, 9). Loss of RFX function causes the absence of cilia, resulting in severe sensory defects in *Caenorhabditis elegans* (10). Piasecki et al. suggested that RFX TFs originated early in the unikont lineage (fungi, Amoebozoa, choanoflagellates, and animals) (11). Transcriptional rewiring of many ciliary genes by RFX TFs occurred early in the animal lineage (11, 12). Thus, RFX TFs co-opted control over the ciliary gene expression in animals, although their DNA-binding domains were conserved (11).

Functional studies of RFX TFs have been performed in several fungal species. For example, in *Penicillium chrysogenum*, PcRFX1 was found to bind to the promoter region of penicillin biosynthetic genes, and knockdown of Pc*rfx1* reduced penicillin production (13). The *cpcR1* gene of *Acremonium chrysogenum* was initially found to bind promoters of cephalosporin C biosynthesis genes. However, disruption of *cpcR1* did not reduce cephalosporin C production (14, 15). Subsequently, it was revealed that *cpcR1* is required for hyphal fragmentation and, thus, for arthrospore formation (16). In *Schizosaccharomyces pombe*, *sak1*$^{+}$ was found to be indispensable for cell viability. Thus, loss of *sak1* caused multiple defects in mitosis and cell morphology (17).

In *Penicillium marneffei*, *rfxA* was found to be essential for cellular division and morphogenesis, particularly during conidiation and yeast growth (18). In

contrast to its action in *S. cerevisiae*, the knockdown mutant of *rfxA* was more sensitive to a DNA damage agent in *P. marneffei*. In *Candida albicans*, *rfx2* repressed genes related to the repair of DNA damage, and regulated hyphal morphogenesis and virulence (5). An *rfx2*-null mutant was shown to be significantly more resistant to UV irradiation than the wild-type strain. In many fungi, RFX TFs have been shown to be required for normal cell division and morphogenesis; however, in *S. cerevisiae*, Sc*rfx1* is dispensable for normal cell growth. Moreover, disruption of RFX TFs causes opposite responses to DNA damage in different fungal species. These findings imply that the functions of RFX TFs are not conserved, despite the presence of a highly conserved DNA-binding domain.

Fusarium graminearum is a major pathogen of Fusarium head blight in wheat, barley, and rice, as well as ear rot and stalk rot in maize. In addition to yield reduction, the fungus contaminates grains with mycotoxins that cause feed refusal and other toxicoses in livestock and pose a threat to food safety (19). *F. graminearum* forms mature perithecia on crop residues and forcibly discharges ascospores, which are the primary inocula (20-23). Conidia produced from sporodochia on infected crops are easily disseminated by rain splash, which act as the secondary inocula (24). Thus, sexual and asexual reproduction of *F. graminearum* are important developmental processes for Fusarium head blight (21) and require the elaborate regulation of many genes (25, 26).

Our research goal was to investigate the role of the RFX TF in *F.*

graminearum. Therefore, the objectives of this study were: (*i*) to identify the RFX TF in *F. graminearum*, (*ii*) to characterize its role in morphogenesis and the DNA-damage response, and (*iii*) to identify RFX TF-regulated genes by analyzing the transcriptome. Results of this study suggest that the transcriptional suppressor *rfx1* is required for maintenance of genome integrity and normal cell growth in *F. graminearum*.

MATERIALS AND METHODS

I. Strains and culture conditions

The *F. graminearum* strains used in this study are listed in Table 1. Standard laboratory methods and culture media for the *Fusarium* species were used (27). Cultures were maintained in complete medium (CM) agar plates. Conidia were produced in carboxymethyl cellulose medium (CMC) or on yeast malt agar (YMA) (28, 29). Unless otherwise stated, the growing temperature of the fungal strains was set at 25°C. All strains were stored as conidia and mycelia in 30% glycerol solution at -80°C.

Conidia were harvested from CMC and transferred to CM containing various DNA-damaging agents at the following concentrations: hydroxyurea (10 mM), methyl methanesulfonate (MMS; 0.1%), and bleomycin (20 mU/ml). Conidia were inoculated on CM agar plates and immediately exposed to UV (254 nm, 480 J/m^2). Germination rates of the conidia were examined by microscopy 18 h after inoculation, and the percentage of germinated conidia was determined. All statistical analyses were conducted using *R* statistical software package (30).

II. Nucleic manipulation, primers, and PCR conditions

Genomic DNA was isolated from lyophilized mycelia, as previously described (27). Restriction endonuclease digestion, Southern blotting, and hybridization with ^{32}P-labeled probes were performed in accordance with standard techniques (31). The PCR primers used in this study were synthesized by an oligonucleotide synthesis facility (Bionics, Seoul, Korea) (Table 2). General PCR procedures were performed in accordance with the manufacturer's instructions (Takara Bio Inc., Otsu, Japan).

Table 1. *F. graminearum* strains used in this study

Name	Genotype	Reference or parents
Z-3639	Wild-type	(58)
Δ*rfx1* strain	Δ*rfx1::gen*	(37)
KH23	Δ*rfx1::rfx1-gfp-hyg*	This study
hH1-GFP strain	*hH1-gfp-hyg*	(59)
Δ*mat1* strain	Δ*mat1-1::gen*	(60)
mat1g	Δ*mat1-1::gen; hH1-gfp-hyg*	(59)
KH24	Δ*rfx1::gen; hH1-gfp-hyg*	mat1g × Δ*rfx1*
mat1r	Δ*mat1-1::gen; hH1-rfp-hyg*	(61)
KH25	Δ*rfx1::rfx1-gfp-hyg; hH1-rfp-hyg*	mat1r × KH23
KH26	Δ*rfx1::gfp-hyg*	This study
KH27	Δ*rfx1::gfp-hyg; hH1-rfp-hyg*	mat1r × KH26
HK12	GFP-*hyg*	(62)

Table 2. Primers used in this study

Primer	Sequence	Description
RFX1/5F	AAAGTTGAGTGATGGTAGGAAGGTAGAGTT	Forward and reverse primers for amplification of 5' flanking region of *rfx1* with tail for the geneticin resistance gene cassette fusion
RFX1/5R	GCACAGGTACACTTGTTTAGAGAGTACAGTTATCCTCTCGTTGGCACAC	
RFX1/3F	CCTTCAATATCATCTTCTGTCGCTCAGAACCAAGGAGAACGAGCAC	Forward and reverse primers for amplification of 3' flanking region of *rfx1* with tail for the geneticin resistance gene cassette fusion
RFX1/3R	CTTCTCGCCAAAGCTGATGACAC	
RFX1/5N	AACACTAAAAGGGGGCATTGGAGA	Forward and reverse nest primers for third fusion PCR for amplification of *rfx1* deletion construct
RFX1/3N	GCTTTGCTGCTGCTGATGGTGA	
Gen/For	CGACAGAAGATGATATTGAAGG	Forward and reverse primers for amplification of geneticin cassette from pII99
Gen/Rev	CTCTAAACAAGTGTACCTGTGC	
Gen-G2	GCAATATCACGGGTAGCCAACG	Forward nest primers for split marker amplication of geneticin resistance gene cassette
Gen-G3	GGGAAGGGACTGGCTGCTATTG	Reverse nest primers for split marker amplication of geneticin resistance gene cassette
RFX1_ORF/Rev	CCAATCCGAGAACATCTGGTTACG	reverse primers for amplification of promoter and ORF region of *rfx1* with tail for GPF tagging
pIGPAPA-sGFP	GTGAGCAAGGGCGAGGAGCTG	Forward and reverse primers for amplification of *gfp-hyg* construct from pIGPAPA
Hyg-F1	GGCTTGGCTGGAGCTAGTGGAGG	

RFX1/3F_GFP	CCTCCACTAGCTCCAGCCAAGCCCTCAG AACCAAGGAGAACGAGCAC	Reverse primers for amplification of 3' flanking region of *rfx1* with tail for GFP tagging
pIGPAPA/H2	TCGCTCCAGTCAATGACCGC	Forward and reverse nest primers for split marker amplication of hygromycin B resistance gene cassette
pU,pBC/H3	CGTTATGTTTATCGGCACTTTGC	Reverse nest primers for split marker amplication of hygromycin B resistance gene cassette
MAT1/5F	GTACTAAGCAAGATCCGAACCACAGC	Forward primer for dominant PCR screening for *MAT1-1-1*
MAT1/with 5F	GTATTGGGGCTTCATTCGGACTTA	Reverse primer for dominant PCR screening for *MAT1-1-1*
RFX1_RT-PCR/For	CGGAGAAATCAACACAGGCAACAG	Forward and reverse primers for qRT-PCR of *rfx1* gene
RFX1_RT-PCR/Rev	TGGGCGAAGCGTAAGGGAATC	
RAD51_RT-PCR/For	TTACAAATCAAGTCGTGGCTCAGG	Forward and reverse primers for qRT-PCR of *rad51* gene
RAD51_RT-PCR/Rev	GAGTCTCAGCTCGACCCTTCTTGA	
Ligase_RT-PCR/For	TCAAAGAGGCCAATGCGAACA	Forward and reverse primers for qRT-PCR of *ligaseIV* gene
Ligase_RT-PCR/Rev	TCTTCTCCGTGGCACCGACTT	
KU80_RT-PCR/For	CAGGACGACGATGGCTATGAGAA	Forward and reverse primers for qRT-PCR of *ku80* gene
KU80_RT-PCR/Rev	GCAACAACAATGGCGGAAACA	
RAD54_RT-PCR/For	ATGGCTGATGAAATGGGACTGG	Forward and reverse primers for qRT-PCR of *rad54* gene
RAD54_RT-PCR/Rev	CGGGACAAACAACAATAGCCTTCT	
RAD52_RT-PCR/For	AGTGTTGGCCTGTCTGTTATTGTCC	Forward and reverse primers for qRT-PCR of *rad52* gene
RAD52_RT-PCR/Rev	ATTCCATCAGTAGTGCCCTCCTTC	
RAD50_RT-PCR/For	GGCGGTTAAAGAGTTGAAGTCCAC	Forward and reverse primers for qRT-PCR of

RAD50_RT-PCR/Rev	TCATTGTACTGAGCCTTGTTTTGGTC	*rad50* gene
KU70_RT-PCR/For	GGACTTTGGATCGCCCGTTATT	Forward and reverse primers for qRT-PCR of *ku70* gene
KU70_RT-PCR/Rev	GCTGTGAAAACTCGACTTGAACCA	
RNR1_RT-PCR/For	CTTGGACAGGGTAGTGGTTGACG	Forward and reverse primers for qRT-PCR of *rnr1* gene
RNR1_RT-PCR/Rev	TGGCAAATGTACAAGAAGGCAGAG	
RNR2_RT-PCR/For	GAGGCAGCGAAGAAAGCAAGAAT	Forward and reverse primers for qRT-PCR of *rnr2* gene
RNR2_RT-PCR/Rev	CCTTGCCTCCTTGTCTCTGCC	

III. Sexual crosses

For self-fertilization, cultures were grown on carrot agar plates for 5 days. Sexual reproduction was induced by removing aerial mycelia with sterile 2.5% Tween 60 solution (27). For outcrosses, female strains grown on carrot agar plates were fertilized with conidial suspension from corresponding male strains 5 days after inoculation. The cultures were incubated under a near-UV lamp (365 nm) at 25°C for an additional 7 days.

IV. Fungal transformation

For green fluorescence protein (GFP) tagging and complementation, a DNA fragment containing the native promoter and the open-reading frame (ORF) of *rfx1* was amplified with RFX1/5F and RFX1_ORF/Rev. The double-joint PCR method (32) was used to fuse the amplicon to the 3'-flanking region of *rfx1* and a GFP cassette containing the hygromycin B resistance gene (*hyg*). Fusion constructs were amplified with nested primers to generate split markers. The resulting constructs were introduced into Δ*rfx1* protoplasts, using the polyethylene glycol-mediated fungal transformation procedure (33). Transformants were selected under hygromycin B (75 μg/ml).

The ORF of *rfx1* was replaced with the GFP cassette to generate KH26 strains (Δ*rfx1::gfp-hyg*). The GFP cassette, 5'-flanking region of *rfx1*, and 3'-flanking region of *rfx1* were fused. The fusion constructs were amplified with nested primers to generate split markers. The resulting constructs were introduced into

wild-type protoplasts. Deletion mutants of *rfx1* were selected under hygromycin B (75 μg/ml) and screened for GFP fluorescence in mycelia.

V. Fluorescence microscopy

Differential interference contrast and fluorescence images were captured on an Axio Imager A1 microscope (Carl Zeiss, Oberkochen, Germany) with a CCD camera. Nuclei of conidia were stained with acriflavin and examined with the 470 nm/525 nm (excitation/emission wavelength) filter set (34). The organelle localizations of RFX1-GFP and histone H1-GFP were imaged with the 470 nm/525 nm filter set. Red fluorescence protein (RFP)-tagged histone H1 was examined with the 550 nm/605 nm filter set. The cell wall was stained with 0.2 μl/ml Calcoflour white (Sigma-Aldrich, St. Louis, MO) and observed using the 550 nm/605 nm filter set. Nuclei were stained with 4',6-diamidino-2-phenylindole (DAPI) (Invitrogen, Carlsbad, CA) and examined with the 365 nm/445 nm filter set (35). Images were analyzed using the AxioVision Rel. 4.7 software package (Carl Zeiss).

VI. Virulence assays

The virulence of fungal strains on wheat head was assessed in the wheat cultivar Eunpamil, as previously described (36, 37). Conidia were harvested from CMC cultures and resuspended to 10^6 spores/ml in 0.01% Tween 20 solution. Mid-anthesis of center spikelet was drop-inoculated with 10 μl of conidial suspension.

Inoculated plants were incubated in a humidity chamber at 25°C for 3 days, and grown in a greenhouse for an additional 18 days. Infected wheat heads were imaged, and the spikelets with head blight symptom were counted.

VII. Toxin analysis

The conidial suspension was inoculated in defined media containing 5 mM of agmatine (MMA) and incubated for 7 days, as previously described (38). Culture filtrates were extracted with an ethyl acetate/methanol mixture (4:1, v/v). The extracts were dried (39), and the residues were derivatized with trimethylsilylating reagent (BSA + TMCS + TMSI, 3:2:3; Supelco, Bellefonte, PA). The resulting samples were analyzed with a Shimadzu QP-5000 gas chromatograph-mass spectrometer (GC-MS; Shimadzu, Kyoto, Japan), as previously described (40).

VIII. Neutral comet assay

Fungal conidia produced in CMC culture were inoculated into 50 ml of YPG liquid medium (3 g of yeast extract, 10 g of peptone, and 20 g of glucose per liter) at 10^6 spores/ml and grown for 12 h with shaking (33). Mycelia were harvested by filtration and incubated in 35 ml of 1 M NH_4Cl containing Driselase (10 mg/ml) (Sigma-Aldrich) at 30°C to generate protoplasts. For bleomycin treatment of wild-type cells, protoplasts were generated in Driselase solution containing 20 mU/ml bleomycin. Protoplasts were collected by centrifugation 4 h after incubation and resuspended in 1 M NH_4Cl.

Low-gelling-temperature agarose (1%; Sigma-Aldrich) was molten in 1 M NH_4Cl and kept at 40°C. The protoplast suspension was mixed with molten agarose at 6×10^3 cells/ml. The agarose was poured on frosted slides and allowed to gel. Slides were submerged in neutral lysis solution for DSB detection, in accordance with a standard protocol (41). After overnight lysis, the slides were washed three times in Tris-acetate-EDTA buffer for 30 min each. Electrophoresis was conducted in Tris-acetate-EDTA buffer for 25 min at 0.6 V/cm. The slides were rinsed with deionized water, stained in ethidium bromide solution, rinsed again with deionized water, and dried at room temperature. Dried agarose gels were rehydrated before fluorescence microscopy.

Comet images were captured on an Axio Imager A1 microscope with a CCD camera and the 550 nm/605 nm filter set. Comet images were composed of the comet head and comet tail. The percentage of DNA in the tail was analyzed for individual comet images by using the CometScore image analysis software (TriTek Corp., Sumerduck,VA).

IX. Quantitative real time (qRT)-PCR

Wild-type and Δ*rfx1* conidia produced in CMC culture were inoculated into 50 ml of CM. The wild-type culture was incubated for 24 h, and the Δ*rfx1* culture was incubated for 32 h with shaking. Mycelia were harvested and subcultured in fresh CM or CM containing 20 mU/ml bleomycin. The cultures were incubated for an additional 2 h. Total RNA was isolated from mycelia that were ground in liquid

nitrogen using an Easy-Spin Total RNA Extraction Kit (Intron Biotech, Seongnam, Korea). First-strand cDNA was synthesized using SuperScript III reverse transcriptase (Invitrogen).

qRT-PCR was performed with a SYBR Green Supermix (Bio-Rad, Hercules, CA) and a 7500 real-time PCR system (Applied Biosystems, Foster City, CA). The endogenous housekeeping gene, ubiquitin C-terminal hydrolase (*ubh*; FGSG_01231.3), was used as a reference gene (42). Transcript levels of target genes under different conditions were compared by the $2^{-\Delta\Delta C_T}$ method (43). qRT-PCR analysis was repeated three times with two biological replications.

X. RNA-sequencing analysis

Wild-type and Δ*rfx1* conidia were harvested from CMC culture and inoculated into CM. The wild-type culture was incubated for 24 h, and the Δ*rfx1* culture was incubated for 32 h with shaking. Total RNA was extracted from mycelia that were ground in liquid nitrogen, as stated above. RNA-sequencing libraries were constructed using the Illumina TruSeq™ RNA sample prep kit, in accordance with the standard low-throughput protocol. Samples were run on an Illumina HiSeq2000 instrument using the reagents provided in the Illumina TruSeq PE Cluster kit V3-cBot-HS and the TruSeq SBS Kit-HS (200 cycles) kit. RNA-sequencing data were deposited in NCBI's Gene Expression Omnibus and are accessible through GEO Series accession number GSE52198.

Genome-wide transcript levels of genes were quantified in reads per kilobase of exon per million mapped sequence reads (RPKM) (44). When the RPKM value was 0, it was changed to 1 to calculate the fold change of transcript level. Genes for which a differential transcript level was detected were functionally characterized using the Munich Information Centre for Protein Sequences FunCat functional classification and annotation system (45). Over-/under-representation analysis of FunCat categories was performed by Pearson's χ^2-test.

RESULTS

I. Molecular characterization of the *rfx1* gene

The *Fusarium* Comparative Database (Fusarium Comparative Sequencing Project, Broad Institute of Harvard and MIT, http://www.broadinstitute.org) annotated the *rfx1* (locus FGSG_07420) based on the presence of an RFX DNA-binding domain. We aligned protein sequences from RFX1 homologs using ClustalW in the MEGA 5.2 program and BoxShade. The alignment showed that the RFX DNA-binding domain of FgRFX1 is highly conserved among all characterized RFX proteins (Fig. 1A). Phylogenetic analyses of RFX homologues were performed using a neighbor-joining algorithm, with bootstrap values calculated from 100 iterations. The phylogenetic tree revealed that RFX homologs of filamentous fungi clustered into a group relative to yeasts and animals (Fig. 1B).

II. Effects of *rfx1* deletion on nuclei and septum formation

The *rfx1* deletion strains were provided by a mutant library of TFs in *F. graminearum* (37). For genetic complementation and GFP tagging of *rfx1*, constructs containing the *rfx1* ORF fused with the GFP cassette were introduced into the deletion mutant. Southern hybridization results showed that the constructs replaced *gen* in the genome of the complementation strains, resulting in KH23 (Fig. 2). The Δ*rfx1* strains showed severely reduced radial growth on CM agar plates and did not produce aerial mycelia (Fig. 3 and Table 3).

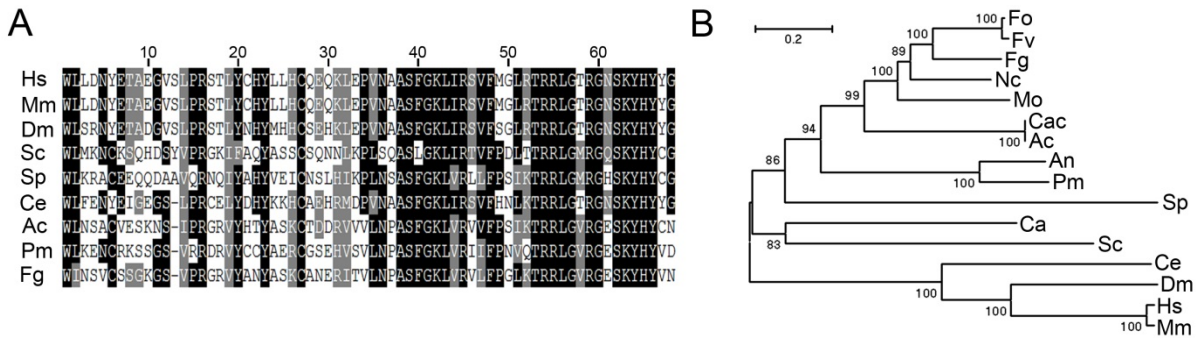

FIG 1. *F. graminearum* RFX1 contains protein motifs characteristic of the RFX protein. (A) Alignment of regions containing the RFX DNA-binding domain from all characterized RFX proteins. (B) Phylogenetic tree of all characterized RFX proteins and fungal putative RFX proteins. Hs, *Homo sapiens*; Mm, *Mus musculus*; Dm, *Drosophila melanogaster*; Sc, *Saccharomyces cerevisiae*; Sp, *Schizosaccharomyces pombe*; Ce, *Caenorhabditis elegans*; Ac, *Acremonium chrysogenum*; Pm, *Penicillium marneffei*; Fg, *F. graminearum*; Fo, *F. oxysporum*; Fv, *F. verticillioides*; Nc, *Neurospora crassa*; Mo, *Magnaporthe oryzae*; Cac, *Cephalosporium acremonium*; An, *Aspergillus nidulans*; Ca, *Candida albicans.*

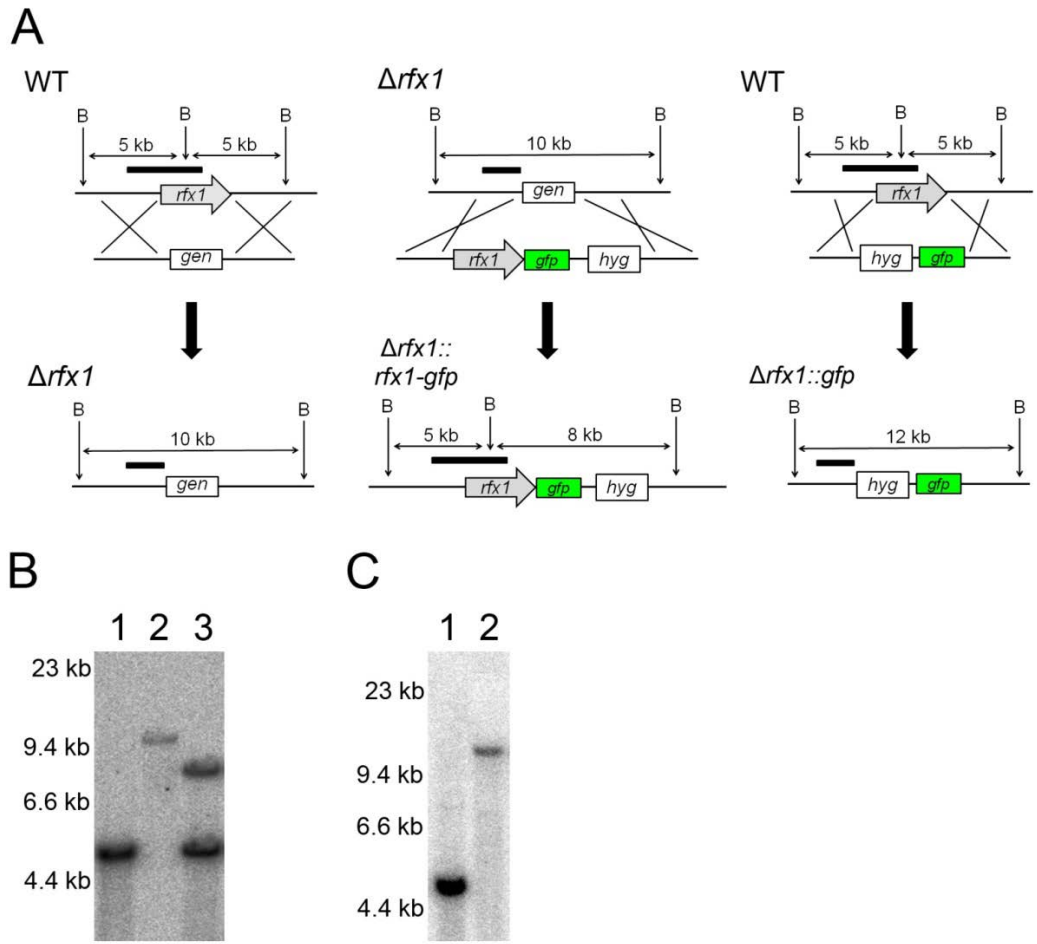
A
WT
Δrfx1
WT
B
5 kb
5 kb
rfx1
gen
10 kb
gen
rfx1
gfp
hyg
5 kb
5 kb
rfx1
hyg
gfp
Δrfx1
Δrfx1::
rfx1-gfp
Δrfx1::gfp
10 kb
gen
5 kb
8 kb
rfx1
gfp
hyg
12 kb
hyg
gfp
B
1 2 3
23 kb
9.4 kb
6.6 kb
4.4 kb
C
1 2
23 kb
9.4 kb
6.6 kb
4.4 kb

Figure 2. Targeted deletion and complementation of *rfx1* gene. **A,** Diagram presenting strategies for deletion, complementation, and replacement with GFP gene of *rfx1*. The 5' flanking regions (black bars) of *rfx1* ORF was used as a probe for hybridization. B, *Bgl*II; *gen*, geneticin resistance gene cassette; *hyg*, hygromycin resistance gene cassette. **B,** Southern blot analysis of deletion and complementation of *rfx1*. Lane 1, wild-type; lane 2, *rfx1* deletion strain; lane 3, complementation strain**. C,** Southern blot analysis of replacement of the *rfx1* gene with the cytoplasmic GFP gene. Lane 1, wild-type; lane 2, *rfx1* deletion strain with cytoplasmic GFP gene. The sizes of the standards (kb) are indicated on the left of each blot.

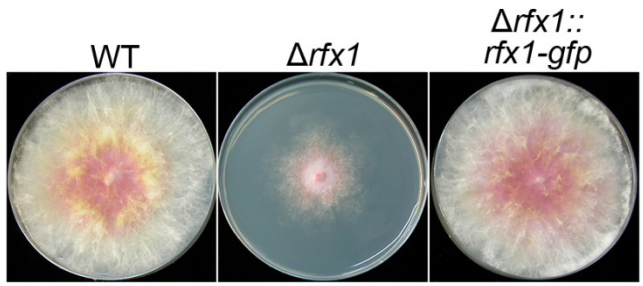

FIG 3. Mycelial growth of fungal strains on complete medium plates. Photographs were taken 4 days after inoculation. WT, wild-type.

Table 3. Vegetative growth, virulence, and trichothecene production in *F. graminearum* strains [a]

Strain type	Radial growth (mm)[b]	Conidium formation (10^5/ml)[c]	Virulence (disease index)[d]	Trichothecene production (mg/g)[e]
Wild-type	39 ± 2.9 [B]	19 ± 4.7 [B]	4 ± 2 [B]	25 ± 2.1 [A]
Δ*rfx1*	21 ± 1.2 [A]	2.4 ± 0.59 [A]	0 ± 0 [A]	20 ± 2.5 [A]
Δ*rfx1::rfx1-gfp*	38 ± 2.2 [B]	17 ± 5.5 [B]	3 ± 2 [B]	21 ± 2.7 [A]

[a] The data presented are average values ± standard deviations. Values within a column with different letters are significantly different ($P < 0.05$) based on Tukey's HSD test.

[b] Radial growth was measured 4 days after inoculation in CM agar plates.

[c] Conidia were counted 5 days after inoculation in CMC.

[d] Disease index (diseased spikelets per wheat head) of the strains was measured 21 days after inoculation.

[e] Total trichothecenes (deoxynivalenol and 15-acetyldeoxynivalenol) were analyzed by a gas chromatograph-mass spectrometer. Trichothecene production was quantified on the basis of the biomass (g) of each sample.

KH24 (Δ*rfx1::gen; hH1-gfp-hyg*) was generated by crossing between mat1g (Δ*mat1-1::gen; hH1-gfp-hyg*) and the Δ*rfx1* strains (Table 1). KH24 showed the same phenotypes as the parental Δ*rfx1* strains and exhibited green fluorescence in nuclei. KH25 (Δ*rfx1::rfx1-gfp-hyg; hH1-rfp-hyg*) was generated by crossing between mat1r (Δ*mat1-1::gen; hH1-rfp-hyg*) and the complementation strains (Δ*rfx1::rfx1-gfp-hyg*). KH25 had both green and red fluorescence in nuclei. Conidia of hH1-GFP, KH24, and KH25 were produced in CMC and inoculated in CM to examine the nuclei and septum formation in hyphae. Mycelia were harvested 12 h after inoculation (except for mycelia of KH24, which were harvested 24 h after inoculation). Septa and nuclei of hyphae were observed by Calcoflour white staining and fluorescent histone H1 proteins, respectively. The formation of septa in Δ*rfx1* hyphae was severely inhibited compared to the wild type (Fig. 4). The Δ*rfx1* hyphae were largely aseptate, whereas wild-type hyphae possessed numerous septa. The Δ*rfx1* nuclei were irregular in size, and Δ*rfx1* produced small fragmented nuclei, called micronuclei.

Conidia production by Δ*rfx1* was 9-times less than that by the wild-type (Table 3). In addition, the Δ*rfx1* conidia were abnormally shaped (Fig. 5). The average conidia length in Δ*rfx1* (71 μm) was much longer than that in the wild-type (45 μm) ($P < 0.01$). Deletion of *rfx1* resulted in more severe defects in the nuclei and septum formation of conidia than those of hyphae. Most wild-type conidia (~70%) had four or five cells, with one nucleus per cell; in contrast, most Δ*rfx1* conidia (~70%) had one or two cells, with multiple nuclei. In the Δ*rfx1* conidia, the

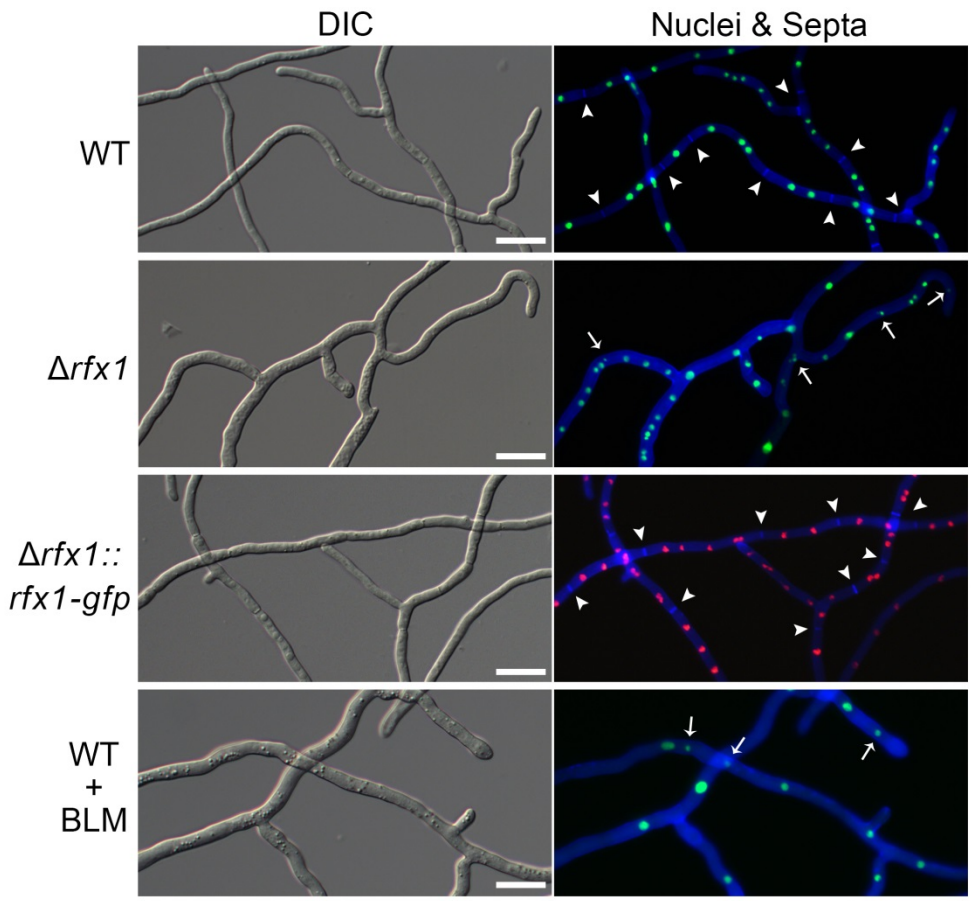

FIG 4. Nuclei and septum formation in hyphae. Histone H1 was tagged with green fluorescence protein (GFP) or red fluorescence protein (RFP) to visualize nuclei. Cell wall was stained with Calcoflour white. Arrowheads indicate septa and arrows indicate micronuclei. Both deletion of *rfx1* and bleomycin treatment inhibit septum formation and produce micronuclei in hyphae. WT, wild-type; WT+BLM, wild-type hyphae grown in 20 mU/ml bleomycin; DIC, differential interference contrast; Nuclei & Septa, overlays of Calcoflour white staining and fluorescence proteins images. Scale bar = 20 μm.

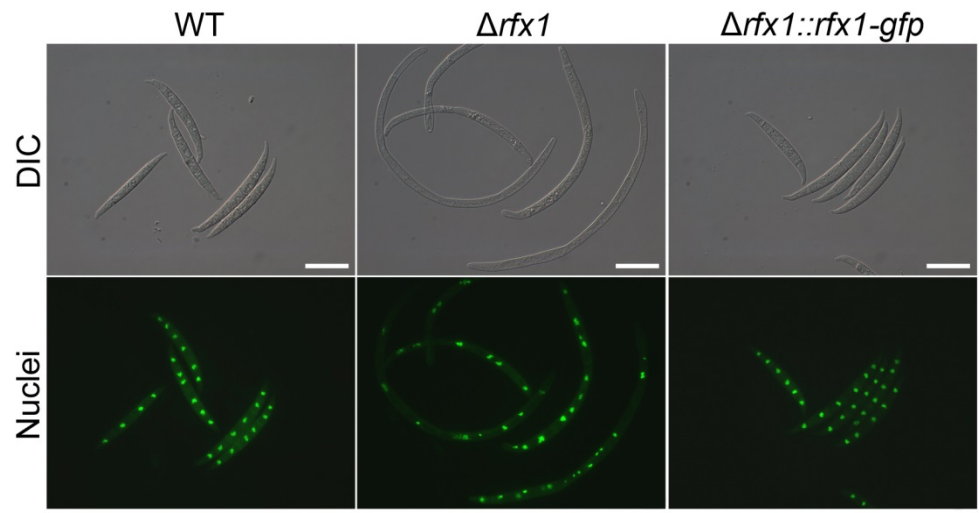

FIG 5. Morphology of Δ*rfx1* conidia changed dramatically. Nuclei in the Δ*rfx1* conidia were fragmented and scattered. WT, wild-type; DIC, differential interference contrast; Nuclei, Acriflavin staining images to visualize nuclei. Scale bar = 20 μm.

nuclei were irregularly shaped and many were micronuclei. The hyphal growth and conidial morphology of KH23 were restored to those of the wild-type strains.

III. Virulence and toxin production

The virulence of the fungal strains was examined by point-inoculation of wheat spikelets. The Δ*rfx1* strains were unable to infect the inoculated spikelets, whereas the wild-type and complemented strains readily colonized the inoculated spikelets and spread to the neighboring spikelets. The disease index (diseased spikelets per wheat head) of the Δ*rfx1* strains was zero (Table 3). We also examined the production of trichothecene, which is an important virulence factor. Trichothecene biosynthesis was induced in MMA, which contains agmatine as a nitrogen source. GC-MS detected two trichothecenes, deoxynivalenol and 15-acetyldeoxynivalenol. The production of total trichothecenes was not markedly different ($P > 0.05$) among the strains on the basis of the biomass (g) of each sample.

IV. Sexual development

The Δ*rfx1* strains produced few immature perithecia, whereas the wild-type and the complementation strains (Δ*rfx1::rfx1-gfp*) produced abundant mature perithecia 7 days after sexual induction (Fig. 6). The perithecia did not contain any ascus structures. Heterothallic *F. graminearum* strains carrying the *MAT1-1* deletion with histone H1-GFP (mat1g) were crossed with Δ*rfx1* mutants to

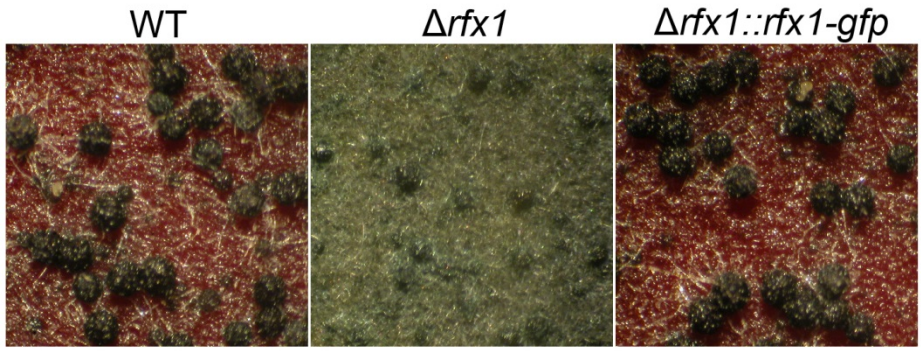

FIG 6. Sexual development of *F. graminearum* strains. Perithecia formed on carrot agar 7 days after sexual induction. WT, wild-type.

investigate the male fertility of the Δ*rfx1* strains. We randomly isolated 144 ascospores, but 57 ascospores did not germinate. Genotypes of the germinated 87 ascospores were analyzed. The segregation ratio of the genotypes was 39:27:8:13 (*rfx1; hH1-gfp* / *rfx1;hH1* / Δ*rfx1;hH1-gfp* / Δ*rfx1;hH1*) indicating that most ascospores carrying the *rfx1* deletion were not viable. Progenies carrying the *rfx1* deletion were much less than those carrying wild-type *rfx1* (21: 66). However, the ratio of hH1-GFP to non-GFP segregation was 1:1, indicating that the outcross underwent normal sexual recombination.

We further investigated the sexual development of *rfx1*, replacing the *rfx1* gene with the cytoplasmic GFP gene, generating Δ*rfx1::gfp-hyg* strains (KH26). KH27 was generated by crossing between mat1r and KH26 (Table 1). Heterothallic *F. graminearum* strains carrying the *MAT1-1* deletion with histone H1-RFP (mat1r) were crossed with KH27 to examine the fertility of the Δ*rfx1* strain as a male (Fig. 7). When mature asci were dissected, four out of eight ascospores expressed GFP, indicating that they were *rfx1* deletion mutants. In *F. graminearum*, ascospores underwent two mitoses, producing four cells with one nucleus after spore delimitation. Ascospores with the *rfx1* deletion were composed of one cell with one or two nuclei, whereas the non-GFP ascospores were composed of four cells with one nucleus. Thus, deletion of *rfx1* blocked mitosis in ascospores after spore delimitation. Defects of spore maturation may cause inviability of ascospores carrying the deletion of *rfx1*.

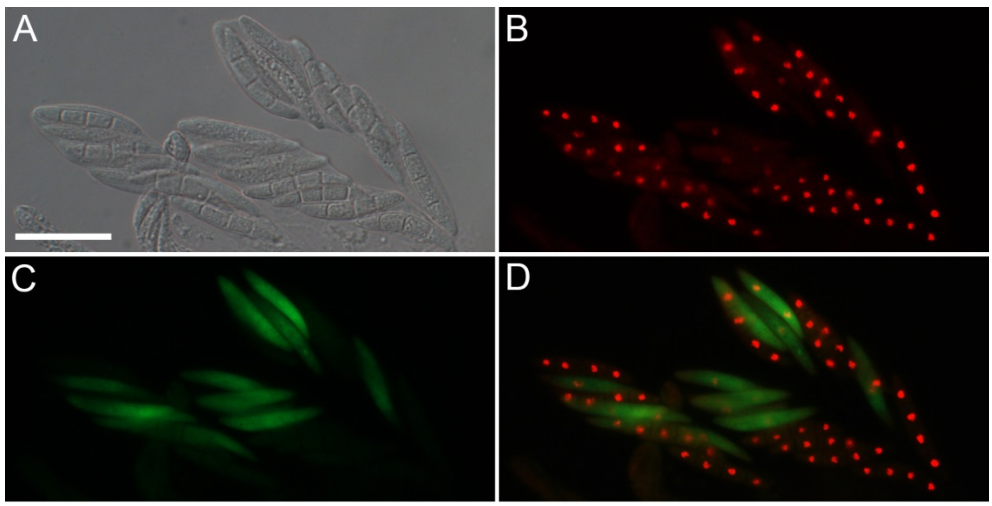

FIG 7. Outcrosses between mat1r (Δ*mat1-1::gen; hH1-rfp-hyg*) female and KH27 (Δ*rfx1::gfp-hyg; hH1-rfp-hyg*) male. In both female and male, histone H1 gene was fused with RFP to visualize nuclei. Ascospores with *rfx1* deletion (GFP-positive) were composed of one cell with one or two nuclei, indicating immaturity. (A) Differential interference contrast. (B) RFP fluorescence image visualizing nuclei. (C) GFP fluorescence image. (D) RFP fluorescence image merged with GFP image. Scale bar = 20 μm.

V. Localization of GFP-tagged RFX1 proteins

To determine the subcellular distribution of RFX1, we complemented the Δ*rfx1* strain by introducing the *RFX1-GFP-hyg* construct, which was GFP-tagged at the C-terminus of RFX1. The resulting Δ*rfx1::rfx1-gfp* strains (KH23) exhibited wild-type phenotypes under all conditions, as previously described. Conidia of KH23 were inoculated in CM and examined after 12 h of incubation. Conidiation of KH23 was induced in CMC and examined 3 days after induction. Although it does not contain any predictable nuclear localization signals, RFX1-GFP localized to the nuclei. Intense fluorescence was found in nuclei of growing hyphae and developing conidiophores (Fig. 8). However, the fluorescence was too weak to detect in mature hyphae and conidia.

VI. Sensitivity of *rfx1* deletion strains to DNA-damage

To investigate the function of *rfx1* in the DNA-damage response, we examined the germination rate of conidia under conditions of DNA damage (Fig. 9). Conidia of the fungal strains were exposed to UV and several DNA-damaging agents, including hydroxyurea, MMS, and bleomycin. The conditions induced low-level DNA damage, such that the wild-type and Δ*rfx1::rfx1-gfp* conidia germinated well. However, the germination rate of Δ*rfx1* conidia was markedly reduced under all DNA-damage conditions, indicating that deletion of *rfx1* resulted in sensitivity to DNA damage, regardless of the damage type.

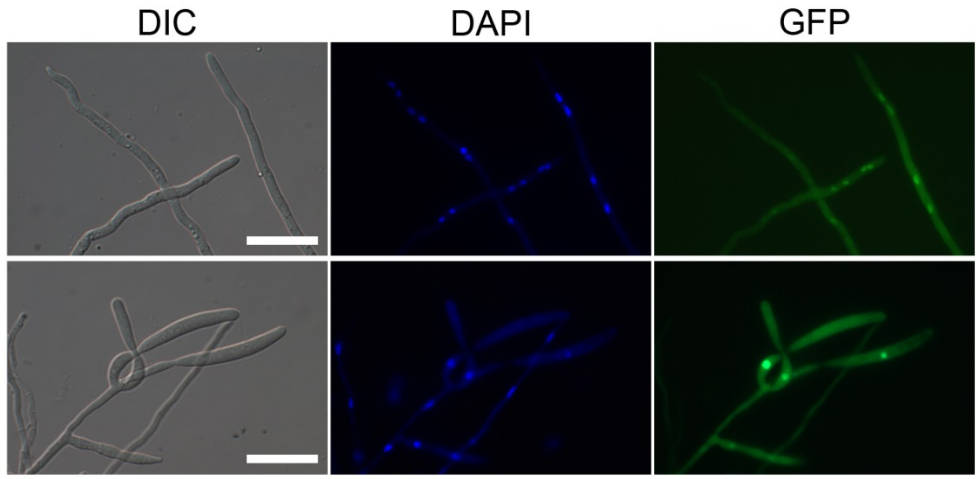

FIG 8. Localization of GFP-tagged RFX1. RFX1-GFP localized into nuclei and exhibited high expression levels in growing hyphae (upper panel) and conidiophores (lower panel). DIC, differential interference contrast; DAPI, DAPI staining images to visualize nuclei; GFP, GFP fluorescence of RFX1-GFP. Scale bar = 20 μm.

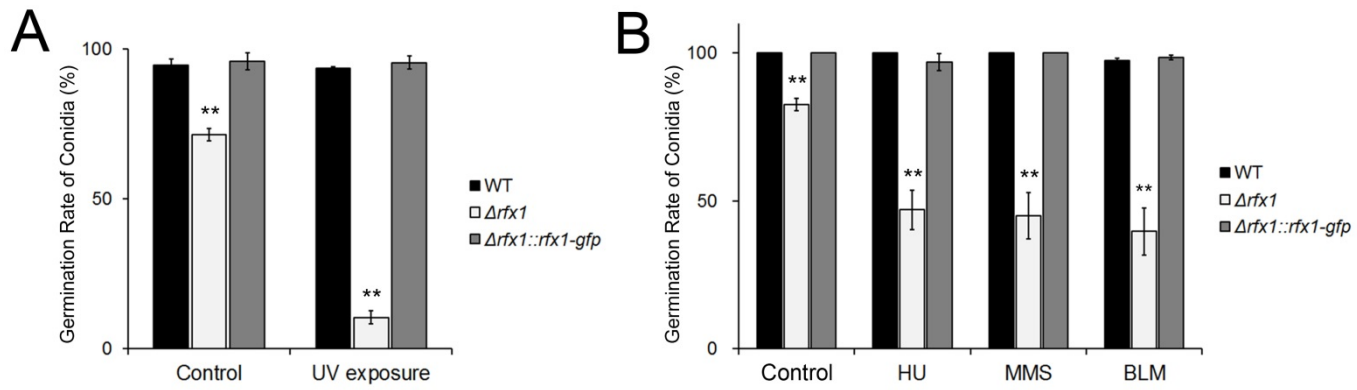

FIG 9. Germination rates of conidia in the DNA-damage condition. (A) Conidia were spread on complete medium agar plates and exposed to UV (254 nm, 480 J/m^2). Germination rates of the conidia were examined under a microscope 18 h after exposure. (B) Conidia were inoculated in complete media containing various DNA-damaging agents (HU, hydroxyurea; MMS, methyl methanesulfonate; BLM, bleomycin). Germination rates of the conidia were determined 18 h after inoculation. Two asterisks show statistically significant differences ($P < 0.01$) from wild-type strain based on independent Student's *t*-test. WT, wild-type; Control, negative control without DNA damage.

Interestingly, we found that bleomycin (10 mU/ml), which induced low levels of DNA damage, inhibited septum formation in the wild-type hyphae. Septum formation was severely delayed and micronuclei were found with a higher concentration (20 mU/ml) of bleomycin (Fig. 4). Bleomycin is known to induce DNA DSBs (46, 47). Both bleomycin and deletion of *rfx1* triggered aseptation and micronuclei in hyphae, implying that deletion of *rfx1* might induce spontaneous DNA strand breaks.

VII. Accumulation of spontaneous DNA DSBs

A neutral comet assay was performed to measure the amount of DNA DSBs in fungal cells. The comet assay combines DNA gel electrophoresis with fluorescence microscopy to visualize the migration of DNA from individual agarose-embedded cells (41). In the neutral comet assay, the comet head contains undamaged DNA, and the comet tail contains DSB-generated fragments. Therefore, cells with more DSBs show a higher percentage of DNA in the tail. Because bleomycin produces DNA DSBs (46, 47), we treated wild-type cells with 20 mU/ml bleomycin as a positive control.

Bleomycin-treated cells contained a higher percentage of DNA in the tail than the untreated cells, indicating that the neutral comet assay detected DNA DSBs (Fig. 10). The percentage of DNA in the tail was increased in Δ*rfx1* cells compared to wild-type cells ($P < 0.01$). Occurrence of DSBs in Δ*rfx1* cells was similar to that

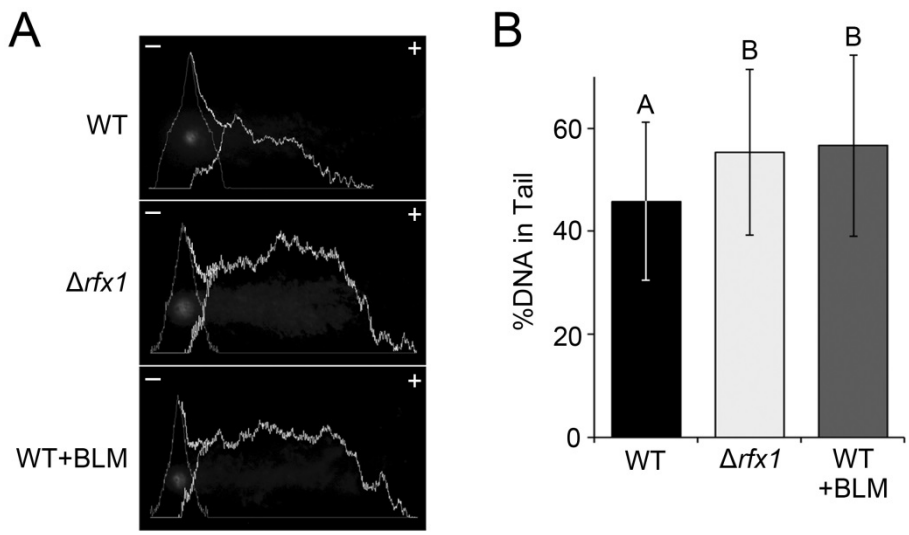

FIG 10. Detection of increased double-strand breaks in Δ*rfx1* cells and bleomycin-treated cells. (A) Photographs of comets and image analysis for neutral comet assay. DNA fragments generated from double-strand breaks migrated toward anode, creating the comet tail. Comets of the Δ*rfx1* and bleomycin-treated cells produced longer tails. Graphs show image analysis quantifying DNA contents of head and tail. (B) Average percentages of DNA in comet tails. The Δ*rfx1* and bleomycin-treated cells exhibited significantly higher percentages of DNA in comet tails than the wild-type ($P < 0.01$).

in bleomycin-treated cells. The results suggested that deletion of *rfx1* triggered DNA DSBs in the absence of a DNA-damaging agent.

VIII. Effects of *rfx1* deletion on genome-wide transcription profiles

We obtained and analyzed genome-wide transcription profiles generated from the RNA-sequencing data of the wild-type and Δ*rfx1* strains. The RPKM values of 13,820 recently re-annotated genes in *F. graminearum* (48) were obtained and compared (DATASET S1, http://ec.asm.org/content/13/3/427). Genes with transcript levels showing a three-fold or greater difference between the Δ*rfx1* and wild-type strains were functionally characterized (45), as shown in Table 4. The results revealed that 38% of all genes were up-regulated in the Δ*rfx1* strains, whereas only 1% were down-regulated. These findings implied roles for RFX1 as a transcriptional repressor. There was a significant enrichment of genes showing a three-fold increase in transcript abundance compared to the genome as a whole ($P < 0.001$) in “Unclassified proteins” category. However, most of the FunCat categories showed significant under-representation of three-fold up-regulated genes ($P < 0.001$) except FunCat 32 and 41. The transcript levels of 35 genes involved in DNA repair (FunCat 10.01.05.01) were increased in the deletion mutants. It implicated that deletion of *rfx1* triggered de-repression of many genes of which functions had not been annotated.

Table 4. Functional categories of genes showing changes in transcripts level in Δ*rfx1* strains compared to the wild-type

		No. genes:		
FunCat ID	**FunCat category name**	**In genome**	**Up-regulated >3-fold**	**Down-regulated >3-fold**
01	Metabolism	2332	801	24
02	Energy	503	139	6
10	Cell cycle and DNA procession	659	85	1
10.01.05.01	DNA repair	156	35	0
11	Transcription	718	26	9
12	Protein synthesis	370	6	1
14	Protein fate	920	106	4
16	Protein with binding function or cofactor requirement	1714	324	10
18	Regulation of metabolism and protein function	242	14	0
20	Cellular transport, transport facilities, and transport routes	1390	411	12
30	Cellular communication/signal transduction mechanism	312	33	1
32	Cell rescue, defense, and virulence	856	312	8
34	Interaction with the environment	606	176	7
40	Cell fate	240	15	0
41	Development	55	18	0
42	Biogenesis of cellular components	617	91	5

43	Cell type differentiation	273	33	1
99	Unclassified proteins	9004	4076	105
-	Total	13820	5300	146

There are two complementary mechanisms for DNA DSB repair: homologous recombination (HR) and non-homologous end-joining (NHEJ). We selected several proteins required for HR and NHEJ (49), including: RAD51, RAD52, and RAD54, which are required for HR; KU70, KU80, and DNA ligase IV, which are required for NHEJ; and RAD50 that is required for both HR and NHEJ. Because Δ*rfx1* cells had spontaneous DNA DSBs, the expression of DSB-repair genes was examined in detail (Table 5). The Δ*rfx1* cells showed greater expression of DSB-repair genes than the wild-type cells in RNA-sequencing analysis.

The transcriptome analyses were validated for the selected genes using qRT-PCR (Table 5). Consistent with the RNA-sequencing data, the DSB-repair genes were up-regulated in the Δ*rfx1* cells in the qRT-PCR analysis. In response to bleomycin, the expression of DSB-repair genes was increased in the wild-type and Δ*rfx1* cells. The Δ*rfx1* cells with bleomycin exhibited highest expression of the genes indicating an additive effect. The finding indicates that both bleomycin and deletion of *rfx1* produced DSBs in DNA and induced expression of DSB-repair genes.

Table 5. Transcripts level of selected genes involved in DNA double-strand break (DSB) repair.

Locus	Putative orthologs of proteins in human[a]	Fold changes of transcript level in RNA-seq[b]	Relative transcript level of indicated strain grown with or without BLM[c]			
			WT		Δ*rfx1*	
			- BLM	+ BLM	- BLM	+ BLM
FGSG_07420 (*rfx1*)	RFX1	0	1.0	0.85	0.0	0.0
FGSG_12711	KU70	7.3	1.0	5.1	4.5	15.1
FGSG_06721	KU80	8.9	1.0	7.9	6.0	24.1
FGSG_04154	DNA Ligase IV	6.3	1.0	2.9	2.6	8.0
FGSG_11814	RAD50	4.6	1.0	1.5	2.7	4.2
FGSG_01157	RAD51	21	1.0	4.6	7.2	17.0
FGSG_10158	RAD52	5.5	1.0	1.8	2.5	3.6
FGSG_07962	RAD54	8.5	1.0	2.5	3.5	5.9
FGSG_05174	RRM1 (RNR1)	2.0	1.0	1.0	1.2	1.2
FGSG_05409	RRM2 (RNR2)	3.4	1.0	0.9	2.1	1.9

[a] The *Fusarium* Comparative Database was searched for homologs of human DSB-repair genes using BLAST analysis.

[b] Fold changes of RPKM values in the Δ*rfx1* strain compared to the wild-type.

[c] Wild-type and Δ*rfx1* mycelia were grown in complete media (CM) and subcultured in fresh CM or CM containing 20 mU/ml of bleomycin (BLM). Cultures were incubated for an additional 2 h, and the total RNA was isolated. Transcript levels of target genes were analyzed by quantitative real time (qRT)-PCR. The endogenous housekeeping gene, ubiquitin C-terminal hydrolase (*ubh*; FGSG_01231.3), was used as a reference gene. Data are expressed as arbitrary units, where the transcript level of the bleomycin-untreated wild-type strains was set to 1.

DISCUSSION

RFXs are conserved TFs in fungi and animals, but their functions appear to have diversified during evolution (11). Several studies have reported that RFX TFs in fungi are required for DNA damage responses, cell division, and differentiation (2, 5, 16-18). The objective of this study was to investigate *rfx1* in *F. graminearum* and to characterize its role in cell morphogenesis and the DNA damage response. We examined deletion mutants of *rfx1* and found that the loss of *rfx1* triggered multiple defects in the fungal life cycle.

The Δ*rfx1* strains lost their pathogenicity in wheat heads (Table 3). As virulence factors of *F. graminearum* in wheat infection, trichothecenes inhibit host defenses (50, 51). Deletion of Fg*rfx1* did not change the production of secondary metabolites, such as pigments and trichothecenes, in *F. graminearum* (Fig. 3 and Table 3). In contrast, knockdown of Pc*rfx1* was shown to reduce penicillin biosynthesis in *P. chrysogenum* (13). Thus, the loss of pathogenicity in this study could not be attributed to trichothecene production. It has been reported that hyphae of *F. graminearum* developed mats and appressoria-like structures to penetrate host cell wall (51). We assume that the Δ*rfx1* strains cannot infect the host cells due to the severe defects in infection-related morphogenesis. The Δ*rfx1* strains were not able to undergo normal morphogenesis in conidiation and sexual development. We hypothesized that deletion of *rfx1* prevented hyphae from developing infection structures required for host infection. Similarly, the

knockdown of *rfxA* resulted in an inability of *P. marneffei* hyphae to transition to infectious yeast cells (18).

Given the role of RFX TFs in response to DNA damage in *S. cerevisiae* (2), it is interesting to speculate whether Fg*rfx1* is involved in a similar mechanism in *F. graminearum*, particularly in light of the increased sensitivity of the Δ*rfx1* strains to DNA damage. UV leads to aberrant covalent bonding between adjacent pyrimidine bases, producing dimers. Hydroxyurea stalls DNA replication because it is an inhibitor of RNRs and thereby depletes dNTP pools (52). The DNA alkylating agent MMS methylates guanine and adenine to cause base mispairing and replication blocks, respectively (53). Bleomycin binds DNA and produces reactive oxygen species that induce DNA DSBs (46, 47). Disruption of Sc*rfx1* increased resistance to UV and MMS in *S. cerevisiae* (5, 6). In *C. albicans*, the *rfx2* deletion mutant was significantly resistant to UV irradiation (5). In this study, deletion of Fg*rfx1* reduced viability to all of these types of DNA damage in *F. graminearum* (Fig. 9). Similarly, knockdown mutants of *rfxA* have been shown to be sensitive to hydroxyurea in *P. marneffei* (18). Phylogenetic analysis showed that Sc*rfx1* and *rfx2* were grouped in the same clade (Fig. 1B). *S. cerevisiae* and *C. albicans* belong to the subphylum Saccharomycotina, while *F. graminearum* and *P. marneffei* are members of the subphylum Pezizomycotina. We suggest that RFX TFs have opposite functions in DNA-damage response between Saccharomycotina and Pezizomycotina. These differences may also reflect specific aspects of the

multinucleate and multicellular growth habit that is characteristic of filamentous hyphae in the Pezizomycotina.

We used the neutral comet assay to demonstrate that Δ*rfx1* cells accumulated DNA DSBs (Fig. 10). RNA-sequencing and qRT-PCR analyses indicated that genes involved in DNA DSB repair were up-regulated in the Δ*rfx1* and bleomycin-treated wild-type strains (Table 5). Bleomycin-treated Δ*rfx1* cells exhibited the highest transcript level of DNA-repair genes, suggesting a synergistic effect. We suggest that spontaneous DSBs resulted in sensitivity of the Δ*rfx1* strains to DNA damage. The mutant cells presumably failed to tolerate additional DNA damage because the integrity of their genomes had already been severely compromised by the loss of RFX1. Although DSB-repair genes were up-regulated in the Δ*rfx1* cells, we suspect that this was insufficient to cope with the DNA damage caused by agents such as bleomycin. Increased sensitivity to DNA damaging agents despite the induction of repair activities has also been observed in the *A. nidulans sepB* mutant (54).

Deletion of *rfx1* inhibited septum formation and produced micronuclei in hyphae and conidia (Fig. 4 and 5). In sexual development, ascospores carrying the *rfx1* deletion did not undergo nuclear division or septation after spore delimitation (Fig. 7). Bleomycin treatment also delayed septum formation and produced micronuclei in *F. graminearum*. Therefore, deletion of *rfx1* likely caused DNA DSBs, which prevented septum formation and produced micronuclei. Micronuclei are biomarkers of chromosomal instability because they result from chromosome

mis-segregation caused by the inability to repair DNA DSBs (55). For example, treatment of *N. crassa* with an inhibitor of DNA topoisomerase I, campothecin, induced micronuclei formation (56). In the present study, low concentration of bleomycin inhibited septation but did not inhibit nuclei division. These observations are consistent with the ability of sublethal doses of hydroxyurea to prevent septum formation in *A. nidulans* (57). However, hydroxyurea and campothecin did not delay septum formation or produce micronuclei in *F. graminearum* (data not shown). These results emphasize the importance of genome integrity in normal cell growth, even if the response to DNA-damaging agents varies between species. In particular, Harris and Kraus suggested that the compartmentalization of hyphae by septa might be exquisitely sensitive to the presence of nuclei that have incurred sub-lethal DNA damage (57). Because compartmentalized nuclei likely represent a source of nuclei that will populate new branches or developmental structures, this response presumably exists to maximize the likelihood that these nuclei are fully intact.

It is apparent that deletion of *rfx1* causes spontaneous DNA DSBs; however, the underlying biochemical mechanism remains to be elucidated. In *S. cerevisiae*, disruption of Sc*rfx1* did not induce DNA DSBs, but rather resistance to DNA damage because of the de-repression of RNRs (5, 6). Transcript levels of the RNR2 homolog were doubled in *F. graminearum* Δ*rfx1* strains compared to the wild-type, whereas the levels of the RNR1 homolog remained stable (Table 5). However, the observed de-repression of RNR2 did not appear to confer resistance to DNA

damage. RFX1-GFP localized in nuclei and exhibited high expression levels in growing hyphae and conidiophores, where nuclear division was actively occurring (Fig. 8). We propose that RFX1 functions as a transcriptional repressor that suppresses many genes involved in DNA-damage repair and cell cycle during normal nuclear division. In accord with this view, RNA-seq analysis showed that deletion of *rfx1* triggered the up-regulation of many genes, including those involved in DNA-damage repair (Table 4 and DATASET S1). The uncontrolled expression of genes in actively growing cells would presumably disrupt DNA replication and chromosome division, generating DNA DSBs.

In conclusion, the *rfx1* gene is important for genome integrity in *F. graminearum*. Disruption of the *rfx1* function resulted in DNA DSBs that, in turn, produced micronuclei and prevented septum formation. Abnormal cell growth caused multiple defects in hyphal growth, conidiation, virulence, sexual development, and the DNA-damage response. These results were different from the yeast model proposed in previous studies (2, 6, 7). In the transcriptional rewiring theory, DNA-binding domains of TFs rarely differ substantially across species, but the target genes regulated by TFs can differ considerably (12). Through transcriptional rewiring, ciliary gene promoters were found to acquire RFX TF regulation early in the animal lineage (11). We propose that RFX1 co-opted control of genes involved in genome integrity by similar process in *F. graminearum*. However, target genes directly regulated by RFX1 have not been identified. Transcriptomic analysis of the Δ*rfx1* strains indicated that *rfx1* directly or indirectly

suppressed more than 5,000 genes. Future work, such as chromatin immunoprecipitation-sequencing, will explore downstream genes that RFX1 binds directly. These studies will help to uncover the function of RFX1 and the evolution of its transcriptional network in fungi.

LITERATURE CITED

1. Zhou B-BS, Elledge SJ. 2000. The DNA damage response: putting checkpoints in perspective. Nature 408:433-439.
2. Huang M, Zhou Z, Elledge SJ. 1998. The DNA replication and damage checkpoint pathways induce transcription by inhibition of the CRT1 repressor. Cell 94:595-605.
3. Chabes A, Georgieva B, Domkin V, Zhao X, Rothstein R, Thelander L. 2003. Survival of DNA damage in yeast directly depends on increased dntp levels allowed by relaxed feedback inhibition of ribonucleotide reductase. Cell 112:391-401.
4. Tanaka H, Arakawa H, Yamaguchi T, Shiraishi K, Fukuda S, Matsui K, Takei Y, Nakamura Y. 2000. A ribonucleotide reductase gene involved in a p53-dependent cell-cycle checkpoint for DNA damage. Nature 404:42-49.
5. Hao B, Clancy CJ, Cheng S, Raman SB, Iczkowski KA, Nguyen MH. 2009. *Candida albicans RFX2* encodes a DNA binding protein involved in DNA damage responses, morphogenesis, and virulence. Eukaryot. Cell 8:627-639.
6. Shen C, Lancaster CS, Shi B, Guo H, Thimmaiah P, Bjornsti M-A. 2007. TOR signaling is a determinant of cell survival in response to DNA damage. Mol. Cell. Biol. 27:7007-7017.
7. Lubelsky Y, Reuven N, Shaul Y. 2005. Autorepression of Rfx1 Gene Expression: Functional Conservation from Yeast to Humans in Response to

DNA Replication Arrest. Mol. Cell. Biol. 25:10665-10673.

8. El Zein L, Ait-Lounis A, Morlé L, Thomas J, Chhin B, Spassky N, Reith W, Durand B. 2009. RFX3 governs growth and beating efficiency of motile cilia in mouse and controls the expression of genes involved in human ciliopathies. J. Cell Sci. 122:3180-3189.

9. Blacque OE, Perens EA, Boroevich KA, Inglis PN, Li C, Warner A, Khattra J, Holt RA, Ou G, Mah AK, McKay SJ, Huang P, Swoboda P, Jones SJM, Marra MA, Baillie DL, Moerman DG, Shaham S, Leroux MR. 2005. Functional genomics of the cilium, a sensory organelle. Curr. Biol. 15:935-941.

10. Swoboda P, Adler HT, Thomas JH. 2000. The RFX-type transcription factor DAF-19 regulates sensory neuron cilium formation in *C. elegans*. Mol. Cell 5:411-421.

11. Piasecki BP, Burghoorn J, Swoboda P. 2010. Regulatory Factor X (RFX)-mediated transcriptional rewiring of ciliary genes in animals. Proc. Natl. Acad. Sci. USA 107:12969-12974.

12. Tuch BB, Li H, Johnson AD. 2008. Evolution of eukaryotic transcription circuits. Science 319:1797-1799.

13. Domínguez-Santos R, Martín J-F, Kosalková K, Prieto C, Ullán RV, García-Estrada C. 2012. The regulatory factor PcRFX1 controls the expression of the three genes of β-lactam biosynthesis in *Penicillium chrysogenum*. Fungal Genet. Biol. 49:866-881.

14. Schmitt EK, Bunse A, Janus D, Hoff B, Friedlin E, Kürnsteiner H, Kück U. 2004. Winged helix transcription factor CPCR1 is involved in regulation of β-lactam biosynthesis in the fungus *Acremonium chrysogenum*. Eukaryot. Cell 3:121-134.

15. Schmitt EK, Kück U. 2000. The fungal CPCR1 protein, which binds specifically to β-lactam biosynthesis genes, is related to human Regulatory Factor X transcription factors. J. Biol. Chem 275:9348-9357.

16. Hoff B, Schmitt EK, Kück U. 2005. CPCR1, but not its interacting transcription factor AcFKH1, controls fungal arthrospore formation in *Acremonium chrysogenum*. Mol. Microbiol. 56:1220-1233.

17. Wu SY, McLeod M. 1995. The sak1+ gene of *Schizosaccharomyces pombe* encodes an RFX family DNA-binding protein that positively regulates cyclic AMP-dependent protein kinase-mediated exit from the mitotic cell cycle. Mol. Cell. Biol. 15:1479-1488.

18. Bugeja HE, Hynes MJ, Andrianopoulos A. 2010. The RFX protein RfxA is an essential regulator of growth and morphogenesis in *Penicillium marneffei*. Eukaryot. Cell 9:578-591.

19. Desjardins AE. 2006. *Fusarium* mycotoxins: chemistry, genetics, and biology. APS Press, St. Paul, MN.

20. Parry DW, Jenkinson P, McLeod L. 1995. *Fusarium* ear blight (scab) in small grain cereals-a review. Plant Pathol. 44:207-238.

21. Fernando WGD, Paulitz TC, Seaman WL, Dutilleul P, Miller JD. 1997.

Head blight gradients caused by *Gibberella zeae* from area sources of inoculum in wheat field plots. Phytopathology 87:414-421.

22. Trail F, Gaffoor I, Vogel S. 2005. Ejection mechanics and trajectory of the ascospores of *Gibberella zeae* (anamorph *Fuarium graminearum*). Fungal Genet. Biol. 42:528-533.

23. Trail F, Xu H, Loranger R, Gadoury D. 2002. Physiological and environmental aspects of ascospore discharge in *Gibberella zeae* (anamorph *Fusarium graminearum*). Mycologia 94:181-189.

24. Jenkinson P, Parry DW. 1994. Splash dispersal of conidia of *Fusarium culmorum* and *Fusarium avenaceum*. Mycol. Res. 98:506-510.

25. Trail F. 2009. For blighted waves of grain: *Fusarium graminearum* in the postgenomics era. Plant Physiol. 149:103-110.

26. Kazan K, Gardiner DM, Manners JM. 2012. On the trail of a cereal killer: recent advances in *Fusarium graminearum* pathogenomics and host resistance. Mol. Plant Pathol. 13:399-413.

27. Leslie JF, Summerell BA. 2006. The *Fusarium* laboratory manual, 1st. Blackwell Publishing, Ames, IA.

28. Cappellini RA, Peterson JL. 1965. Macroconidium formation in submerged cultures by a non-sporulating strain of *Gibberella zeae*. Mycologia 57:962-966.

29. Harris SD. 2005. Morphogenesis in germinating *Fusarium graminearum* macroconidia. Mycologia 97:880-887.

30. R Core Team. 2012. R: A language and environment for statistical computing. R Foundation for Statistical Computing, Vienna, Austria.

31. Sambrook J, Russell DW. 2001. Molecular cloning : a laboratory manual, 3rd. Cold Spring Harbor Laboratory Press, Cold Spring Harbor, N.Y.

32. Yu JH, Hamari Z, Han KH, Seo JA, Reyes-Dominguez Y, Scazzocchio C. 2004. Double-joint PCR: a PCR-based molecular tool for gene manipulations in filamentous fungi. Fungal Genet. Biol. 41:973-981.

33. Lee T, Han Y-K, Kim K-H, Yun S-H, Lee Y-W. 2002. *Tri13* and *Tri7* determine deoxynivalenol- and nivalenol-producing chemotypes of *Gibberella zeae*. Appl. Environ. Microbiol. 68:2148-2154.

34. Raju NB. 1986. A simple fluorescent staining method for meiotic chromosomes of *Neurospora*. Mycologia 78:901-906.

35. Seong K-Y, Zhao X, Xu J-R, Güldener U, Kistler HC. 2008. Conidial germination in the filamentous fungus *Fusarium graminearum*. Fungal Genet. Biol. 45:389-399.

36. Lee S-H, Lee J, Lee S, Park E-H, Kim K-W, Kim M-D, Yun S-H, Lee Y-W. 2009. *GzSNF1* is required for normal sexual and asexual development in the ascomycete *Gibberella zeae*. Eukaryot. Cell 8:116-127.

37. Son H, Seo Y-S, Min K, Park AR, Lee J, Jin J-M, Lin Y, Cao P, Hong S-Y, Kim E-K, Lee S-H, Cho A, Lee S, Kim M-G, Kim Y, Kim J-E, Kim J-C, Choi GJ, Yun S-H, Lim JY, Kim M, Lee Y-H, Choi Y-D, Lee Y-W. 2011. A phenome-based functional analysis of transcription factors in the cereal

head blight fungus, *Fusarium graminearum*. PLoS Pathog. 7:e1002310.

38. Gardiner DM, Kazan K, Manners JM. 2009. Novel genes of *Fusarium graminearum* that negatively regulate deoxynivalenol production and virulence. Mol Plant-Microbe Interact 22:1588-1600.

39. He J, Yang R, Zhou T, Tsao R, Young JC, Zhu H, Li X-Z, Boland GJ. 2007. Purification of deoxynivalenol from *Fusarium graminearum* rice culture and mouldy corn by high-speed counter-current chromatography. J. Chromatogr. A 1151:187-192.

40. Seo J-A, Kim J-C, Lee D-H, Lee Y-W. 1996. Variation in 8-ketotrichothecenes and zearalenone production by *Fusarium graminearum* isolates from corn and barley in Korea. Mycopathologia 134:31-37.

41. Olive PL, Banath JP. 2006. The comet assay: a method to measure DNA damage in individual cells. Nat. Protocols 1:23-29.

42. Kim HK, Yun SH. 2011. Evaluation of potential reference genes for quantitative RT-PCR analysis in *Fusarium graminearum* under different culture conditions. Plant Pathology J. 27:301-309.

43. Livak KJ, Schmittgen TD. 2001. Analysis of relative gene expression data using real-Time quantitative PCR and the $2^{-\Delta\Delta CT}$ Method. Methods 25:402-408.

44. Mortazavi A, Williams BA, McCue K, Schaeffer L, Wold B. 2008. Mapping and quantifying mammalian transcriptomes by RNA-Seq. Nat. Meth. 5:621-628.

45. Ruepp A, Zollner A, Maier D, Albermann K, Hani J, Mokrejs M, Tetko I, Güldener U, Mannhaupt G, Münsterkötter M, Mewes HW. 2004. The FunCat, a functional annotation scheme for systematic classification of proteins from whole genomes. Nucleic Acids Res. 32:5539-5545.

46. Povirk LF, Wübker W, Köhnlein W, Hutchinson F. 1977. DNA double-strand breaks and alkali-labile bonds produced by bleomycin. Nucleic Acids Res. 4:3573-3580.

47. Stubbe J, Kozarich JW. 1987. Mechanisms of bleomycin-induced DNA-degradation. Chem. Rev. 87:1107-1136.

48. Wong P, Walter M, Lee W, Mannhaupt G, Münsterkötter M, Mewes H-W, Adam G, Güldener U. 2011. FGDB: revisiting the genome annotation of the plant pathogen *Fusarium graminearum*. Nucleic Acids Res. 39:D637-D639.

49. Khanna KK, Jackson SP. 2001. DNA double-strand breaks: signaling, repair and the cancer connection. Nat. Genet. 27:247-254.

50. Desjardins AE, Proctor RH, Bai GH, McCormick SP, Shaner G, Buechley G, Hohn TM. 1996. Reduced virulence of trichothecene-nonproducing mutants of *Gibberella zeae* in wheat field tests. Mol. Plant-Microbe Interact. 9:775-781.

51. Jansen C, von Wettstein D, Schäfer W, Kogel K-H, Felk A, Maier FJ. 2005. Infection patterns in barley and wheat spikes inoculated with wild-type and trichodiene synthase gene disrupted *Fusarium graminearum*. Proc. Natl.

Acad. Sci. USA 102:16892-16897.

52. Koç A, Wheeler LJ, Mathews CK, Merrill GF. 2004. Hydroxyurea arrests DNA replication by a mechanism that preserves basal dNTP pools. J. Biol. Chem. 279:223-230.

53. Lundin C, North M, Erixon K, Walters K, Jenssen D, Goldman ASH, Helleday T. 2005. Methyl methanesulfonate (MMS) produces heat-labile DNA damage but no detectable in vivo DNA double-strand breaks. Nucleic Acids Res. 33:3799-3811.

54. Gygax SE, Semighini CP, Goldman GH, Harris SD. 2005. $SepB^{CTF4}$ is required for the formation of DNA-damage-induced $UvsC^{RAD51}$ foci in *Aspergillus nidulans*. Genetics 169:1391-1402.

55. Fenech M, Kirsch-Volders M, Natarajan AT, Surralles J, Crott JW, Parry J, Norppa H, Eastmond DA, Tucker JD, Thomas P. 2011. Molecular mechanisms of micronucleus, nucleoplasmic bridge and nuclear bud formation in mammalian and human cells. Mutagenesis 26:125-132.

56. Wakabayashi M, Ishii C, Hatakeyama S, Inoue H, Tanaka S. 2010. ATM and ATR homologes of *Neurospora crassa* are essential for normal cell growth and maintenance of chromosome integrity. Fungal Genet. Biol. 47:809-817.

57. Harris SD, Kraus PR. 1998. Regulation of septum formation in *Aspergillus nidulans* by a DNA damage checkpoint pathway. Genetics 148:1055-1067.

58. Bowden RL, Leslie JF. 1999. Sexual recombination in *Gibberella zeae*.

Phytopathology 89:182-188.

59. Hong S-Y, So J, Lee J, Min K, Son H, Park C, Yun S-H, Lee Y-W. 2010. Functional analyses of two syntaxin-like SNARE genes, *GzSYN1* and *GzSYN2*, in the ascomycete *Gibberella zeae*. Fungal Genet. Biol. 47:364-372.

60. Lee J, Lee T, Lee Y-W, Yun S-H, Turgeon BG. 2003. Shifting fungal reproductive mode by manipulation of mating type genes: obligatory heterothallism of *Gibberella zeae*. Mol. Microbiol. 50:145-152.

61. Son H, Lee J, Park AR, Lee Y-W. 2011. ATP citrate lyase is required for normal sexual and asexual development in *Gibberella zeae*. Fungal Genet. Biol. 48:408-417.

62. Son H, Min K, Lee J, Raju NB, Lee Y-W. 2011. Meiotic silencing in the homothallic fungus *Gibberella zeae*. Fungal Biol. 115:1290-1302.

요약 (국문초록)

*Fusarium graminearum*의 전사조절인자 RFX1의 기능연구

민경훈

세포로 이루어진 생물들의 생존은 DNA의 정확한 복제와 전달에 달려있다. Regulatory factor X (RFX) 전사조절인자들은 동물과 곰팡이계에서 잘 보존되어 있다. 하지만 이들의 기능은 DNA 손상수리에서부터 섬모유전자 조절에 이르기까지 다양하다. 우리는 식물병원성 곰팡이 *Fusarium graminearum*에 존재하는 RFX 전사조절인자, RFX1의 기능을 연구하였다. *rfx1* 유전자를 삭제하였을 때 곰팡이의 균사생장, 분생포자 형성, 병원성, 유성생식 등에서 다양한 장애가 발생하였다. *rfx1* 삭제균주는 여러가지 종류의 DNA 손상에 야생형보다 취약하였다. 또한 삭제균주에서 격벽의 생성이 억제되고 미소핵 (micronuclei)가 형성되었다. Neutral comet assay를 수행한 결과, *rfx1*의 기능을 방해하였을 때 자발적인 DNA 이중나선 손상 (double-strand break)이 일어난다는 것을 발견하였다. 그로인해 DNA 이중나선 손상을 수리하는 유전자들의

발현이 *rfx1* 삭제균주에서 증가하였다. *F. graminearum*에서 DNA 이중나선 손상은 미소핵을 만들어내고 격벽의 형성을 억제하였다. 형광단백질 (GFP)를 표지한 RFX1 단백질은 세포핵에 위치하였다. 특히 핵분열이 왕성하게 일어나고 있는 균사와 분생자꼭지 (conidiophore)에서 RFX1-GFP 단백질이 강하게 발현되었다. RNA-sequencing을 기반으로 한 전사체 분석 결과, RFX1은 DNA 손상 수리 유전자들을 포함한 많은 수의 유전자들의 발현을 억제하고 있었다. 이러한 결과들은 전사억제자 *rfx1*가 게놈의 온전성을 유지함으로써, 곰팡이가 정상적인 세포생장을 하는데 꼭 필요하다는 것을 보여준다.

주요어: 붉은곰팡이, 전사조절인자, RFX1, DNA 이중나선 손상, 세포 분열, RNA-sequencing

학번: 2008-23080